Fronteiras: Journal of Social, Technological and Environmental Science
http://periodicos.unievangelica.edu.br/fronteiras/
ISSN 2238-8869

Article

Design and Analysis of Math function Based Controller Combined with Neural Network Applied to the Solar-Powered Electric Vehicle

Raghavaiah Katuri [1] *, Srinivasa Rao Gorantla [2]

[1] Department of Electrical Engineering, Vignan's Foundation for Science Technology and Research Deemed to be University, Vadlamudi, Guntur, Andhra Pradesh, India; ORCID: 0000-0002-3315-1900; E-mail: k_eeep@vignanuniversity.org

[2] Professor Department of Electrical Engineering, Vignan's Foundation for Science Technology and Research Deemed to be University, Vadlamudi, Guntur, Andhra Pradesh, India; ORCID: 0000-0002-9033-7437; E-mail: srm.gorantla@gmail.com

*Correspondence: Phone Number: +919014362427, e-mail: k_eeep@vignanuniversity.org

ABSTRACT

The transition between the battery and ultracapacitor (UC) according to the driver requirements is the key obstacle that is related to the hybrid energy storage system (HESS) powered electric vehicles (EVs). In this effort, an innovative control scheme has been proposed, to switch the power sources corresponding to the vehicle dynamics. An MFB controller is considered with 4- math functions and programmed independently. Thereafter, a new hybrid controller has been formed by joining the designed MFB controller with an artificial neural network (ANN) to achieve the precise transition between battery and UC. The battery gets charged from the photovoltaic (PV) panel corresponding to the irradiance and temperature availability. The charging and discharging periods of battery mainly depending upon the control switches (CS) present in the circuit. From those two controllers, ANN generates required switching pulses whereas the MFB controller regulates the pulse depending upon the speed of the motor. Finally, the combination of MFB with ANN controller produces the required pulse signals to switches present in unidirectional (UDC) and bidirectional converter (BDC) related to the speed of the motor. The MATLAB/Simulink model of the system is done in four modes with different loads, and all results are discussed in the simulation and results section.

Keywords: HESS; solar power; artificial neural network (ANN) controller; math unction based (MFB) controller.

RESUMO

A transição entre a bateria e o ultracapacitor (UC), de acordo com os requisitos do motorista, é o principal obstáculo relacionado aos veículos elétricos (VEs) movidos pelo sistema híbrido de armazenamento de energia (HESS). Nesse esforço, um inovador esquema de controle foi proposto, para alternar as fontes de energia correspondentes à dinâmica do veículo. Um controlador MFB é considerado com 4 funções matemáticas e programado de forma independente. Posteriormente, um novo controlador híbrido foi formado juntando o controlador MFB projetado a uma rede neural artificial (RNA) para alcançar a transição precisa entre a bateria e a UC. A bateria é carregada no painel fotovoltaico (PV) correspondente à irradiância e disponibilidade de temperatura. Os períodos de carga e descarga da bateria dependem principalmente dos interruptores de controle (CS) presentes no circuito. A partir desses dois

Submissão: 01/09/2018 Aceite: 29/03/2022 Publicação: 29/04/2022

v.11, n.1, jan. - abr. 2022 • p. 315-332. • DOI http://dx.doi.org/10.21664/2238-8869.2022v11i1.p315-332.

controladores, a ANN gera pulsos de comutação necessários, enquanto o controlador MFB regula o pulso dependendo da velocidade do motor. Finalmente, a combinação do MFB com o controlador ANN produz os sinais de pulso necessários para os interruptores presentes no conversor unidirecional (UDC) e bidirecional (BDC) relacionados à velocidade do motor. O modelo MATLAB / Simulink do sistema é realizado em quatro modos com cargas diferentes, e todos os resultados são discutidos na seção de simulação e resultados.

Palavras-chave: HESS; energia solar; controlador de rede neural artificial (RNA); controlador baseado em unção matemática (MFB).

1. Introduction

In recent days people are concentrated on developing an eco-friendly transportation system because, the conventional transportation system creating much pollution in the atmosphere. EVs are developed after serval decades to reduce the pollution that might be air or sound pollution. Conventionally majority of EVs are power with battery and which will have some drawbacks like driving range as well as low power density. Thereafter HESS based electric vehicle to avoid some of the draws associated with conventional EVs. The HESS was developed by combining battery with UC; here UC doesn't have high energy density so it could not use for continuous power supply to the load. To obtain the proper power-sharing between two energy sources according to the electric vehicle requirement several conventional as well as intelligent controllers developed. Proper power splitting of HESS during real-time implementation is the major challenge associated with electric vehicles. A rule-based energy management strategy has been proposed to obtain the optimized energy sharing between the battery and UC also considered the dc-dc converter with less switching losses (Shen, J. et.al).

The EVs are designed with solar power-assisted battery, which indicates that the battery of the EV gets charged from the solar power. In solar balancing, mode battery gets charged from solar power, in storage balancing mode battery charged from conventional power storage at that time of stoppage of a vehicle, and in charge balancing mode battery can discharge the power to the load (Duan, C. et.al). Generally, for implementing solar to vehicle charging strategy integration is one of the difficult factors related to EVs. Swapping of the batteries from battery stations to the vehicle can be done for vehicle propulsion. Battery storage systems are runs with solar power as well as conventional power, to develop the independence of EVs self-charge mechanism was developed with solar which is inbuilt integrated into the vehicle. With this arrangement battery of the EV can charge from the vehicle panel during sunlight available time (Liu, N.et.al).

Asymmetric bidirectional Z-source topology was proposed for HESS based EVs for proper power balancing between battery and UC. With the developed topology maximum utilization of UC can be achieved (Hu, S. et.al). Optimal allocations of the solar plants benefit the economy of the industry. This optimal allocation is also a very difficult factor due to the continuous changing condition of utilization as well as the availability of sunlight (Ghiassi-Farrokhfal.et.al). Due to low kinetic dynamics of the vehicle battery internal resistance can be increased this cause to the reduction of the capacity of the source; to overcome this HESS is introduced with different practical cases (Keil, P. et.al). For improving the life of the battery superconducting magnetic energy storage was considered and combined, made HESS. The designed HESS system enhances the electric bus performance by increasing the life of the battery and dismissing the size of the storage system (Li, J. et.al).

Two different real-time controllers are developed to share the power to battery and UC which will use to protect the state of health of the battery. Based on Karush–Kuhn–Tucker conditions one controller is designed and another one is designed based on the neural network. Further developed two controllers are implemented in real-time to electric vehicles (Shen, J.et.al). For a specific electric vehicle point of view, HESS is introduced by combining battery with a supercapacitor and smart energy as well as power-sharing can be achieved by the fuzzy logic control system (Trovao, J.et.al). Electric vehicle charging stations are one of the major issues with well-developed countries. Generally, all-EVs are charged from the local plug-in charging stations which will create an extra burden on the power grid, which means there is an internal deficiency that occurs in the distribution system. In order to avoid that situation PV based power generation is incorporated with the electric vehicle itself and utilized the power whenever the sunlight is available. If

sunlight is not available then the electric vehicle can be charged from the conventional grid, all this can be achieved with an optimized algorithm (Chaudhari, K. et.al).

In HESS powered electric vehicles smart energy management is one of the major challenges. Particle swarm optimization incorporating the Nelder–Mead simplex technique is proposed to make the possibility of smart energy management between the battery and UC (Mesbahi, T.et.al). A nonlinear model predictive control was developed for splitting the energy between supercapacitor and battery (Golchoubian, P.et.al). Most of the countries in the world are concentrating on developing an electric vehicle which will create an extra burden on the local substations. Solar power stations are developed along with conventional grids and the PV system also included within the vehicle itself for a better driving range of the electric vehicle (Khan, S. et.al).

The main objective of this work is to develop a new control strategy (MFB puls ANN) by combining the considered MFB controller with the ANN controller. The suggested control strategy works related to the speed of the motor without showing much effect on the remaining devices. This entire work can be organized with chapters in that the proposed model can be illustrated in chapter two. Chapter three includes PV array mathematical modeling. Chapter four Chapter six says about the overview of the BLDC motor. In chapter five describes the artificial neural network controller. Chapter six includes modes of operation of proposed HESS. Proposed control (MFB puls ANN) approach described in chapter seven. Simulation and results are described in chapter eight. Finally, the conclusions part can be described in chapter nine.

2. Proposed model

The proposed scheme can be represented with figure 1 and this mainly comprising of HESS, controllers, converters and solar panels to drive EV. Here three CS's are associated between the PV panel to the battery, PV panel UDC and battery to UDC. The SOC (state of charge) of the battery and output voltage of the PV panel decides the ON/OFF states of the three CS's. The designed MFB controller and ANN controller together work and make the pulses to BDC and UDC related to the speed of EV. The ANN controller develops the control signal to the converter switches, whereas the MFB controller controls that signal corresponding to the speed of the motor. The UC supplies the transient power of the motor, which means UC assists the battery during peak load conditions and starting of the EV.

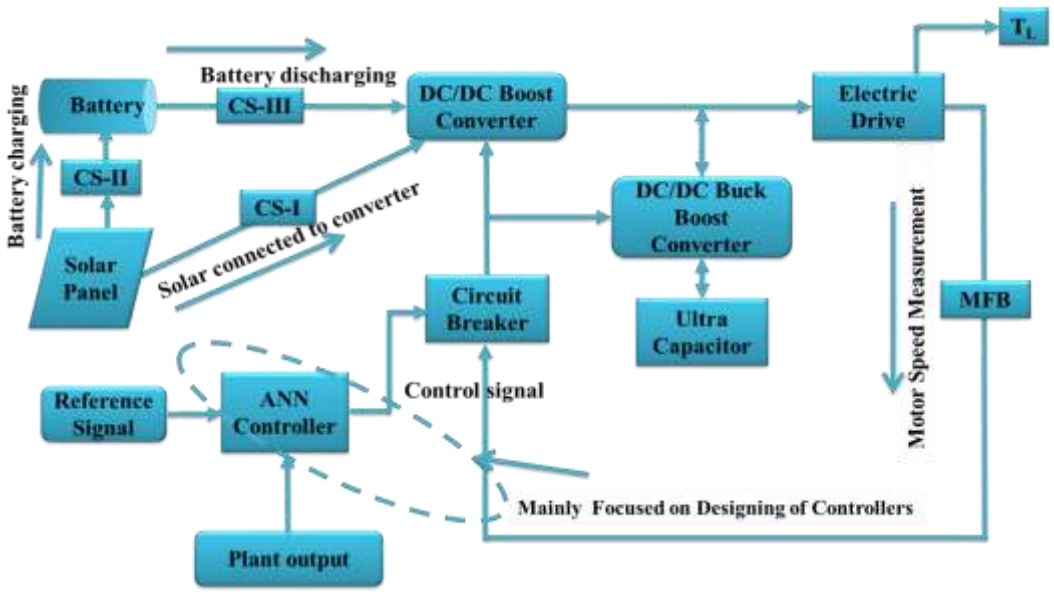

Figure 1. Proposed model block diagram representation

Converter's main circuit model is shown in figure 2; here the battery is connected at UDC end whereas UC has connected at BDC end. And two converters comprised of MOSFET switches. During boost operation of UDC, the switch S_1 is in ON position

whereas during boost operation of BDC switch S_3 is in ON condition, and during buck operation of BDC switch S_2 is in ON state. The PV panel is used to charge the battery and connected to the UDC directly, to propel the electric drive.

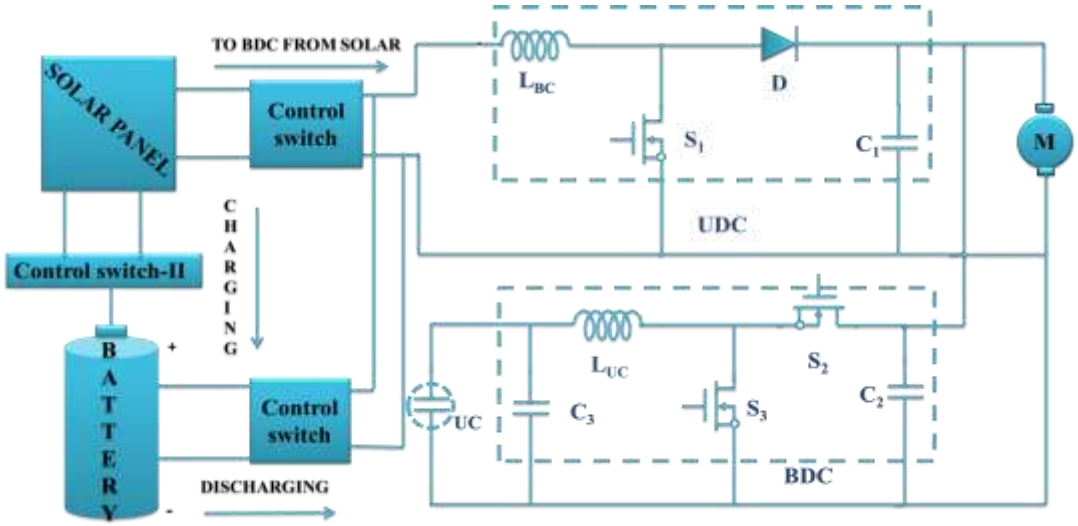

Figure 2. Converter model main circuit diagram with a solar panel

3. Mathematical Modelling of PV Array

The PV cell is capable of produce a voltage of 0.7 V, 0.5 V during the open circuit, and normal working conditions. To make a single PV module, several PV cells should connect in series and parallel combinations. The PV system is formed using modules and which can produce output power with 15% efficiency. Figure 3(a) representing the ideal PV cell structure. Figure 3(b), 3(c) shows the equivalent short circuit and open circuit model of the PV cell.

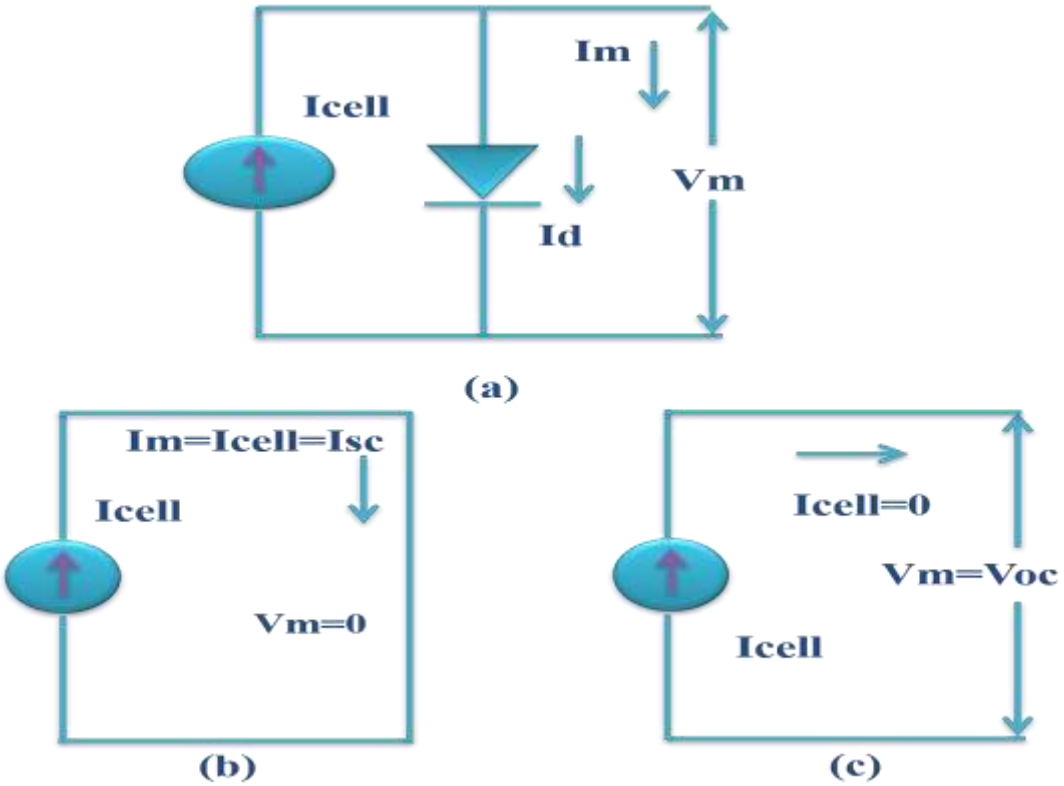

Figure 3. (a) Conventional PV model, (b) short-circuited PV model (c) open-circuited PV model

From figure 3(a) the current source cell current I_{cell} is divided as diode current Id and load current I_m. From figure 3(b), three current I_{cell} Id and Im are all are the same due to short-circuited output. In the same way the output voltage of the cell V_m is equal to the open-circuit voltage V_{oc}.

To find the output current of the cell, apply Kirchhoff voltage law (KVL) to figure 3(a)

$$\boldsymbol{I_m = I_{cell} - I_d} \quad ----------(1)$$

The diode current is

$$\boldsymbol{I_d = I_{rscell}\left[e^{\left(\frac{QV}{KTap}\right)-1}\right]} \quad ----------(2)$$

PV model current-voltage equation becomes

$$\boldsymbol{I_m = I_{cell} - I_{rscell}\left[e^{\left(\frac{QV}{KTap}\right)-1}\right]} \quad --------\ (3)$$

Finally, diode reverse saturation current can be obtained

$$\boldsymbol{I_{rscell} = \frac{I_{cell}}{\left[e^{\left(\frac{QV}{KTap}\right)-1}\right]}} \quad ----------(4)$$

4. About Brushless Direct Current (BLDC) Electric Motor

In this section the general view of the electric motor with specifications is discussed. Because the electric motor plays key during the manufacturing of the EV. In this work, the BLDC motor is considered for the successful operation of the EV. The BLDC motor is one having stator and rotor, in which the rotor is constructed with electromagnets and stator is constructed with permanent magnets. No brushes are used in this motor construction and which increases the efficiency, performance compares to other electric motors.

Table 1. BLDC motor parameter

s.no	Parameter name	Value
1	Rated voltage	12 V
2	Rated power	200 W
3	Rated speed	5000 Rpm
4	Rated current	16.66 A
5	Rated torque	0.4 Nm

5. About the ann Controller

In this work, the ANN controller is used to transform the nonlinear system changing aspects into linear dynamics by canceling the nonlinearities. The controller is just a reorganization of the neural network plant model. First, the plant model was trained thereafter implemented to the proposed control strategy scheme. Here BDC and UDC considered as a plant model. The discrete model of an ANN controller is

$$\boldsymbol{y(k+1) = f[y(k), y(k-1), \ldots . y(k-n+1), u(k-1), \ldots . u(k-m+1)]}$$
$$\boldsymbol{+ g[y(k), y(k-1), \ldots . , y(k-n+1), u(k-1), \ldots . u(k-m+1)].u(k)} \quad --(5)$$

Here $\boldsymbol{f(.)}$ and $\boldsymbol{g(.)}$ are the additive non-linear term and g(.) the multiplicative non-linear term

The control law is given as

$$\boldsymbol{u(k) = \frac{y_r(k+1) - f[y_n(k), u_m(k-1)}{g[y_n(k), u_m(k-1)]}} \quad -----(6)$$

$$\boldsymbol{y_n(k) = [u(k-1), u(k-2), \ldots . , u(k-m)]^T} \quad ----(7)$$

Here $\boldsymbol{y_r(k+1)}$ is the reference signal to be tracked. Applying the Control Law to the ANN model results "y" follows $\boldsymbol{y_r}$ exactly and that can be represented with equation number (8)

$$\boldsymbol{y(k+1) = y_r(k+1) - - - - - - - - - - - - - - - - (8)}$$

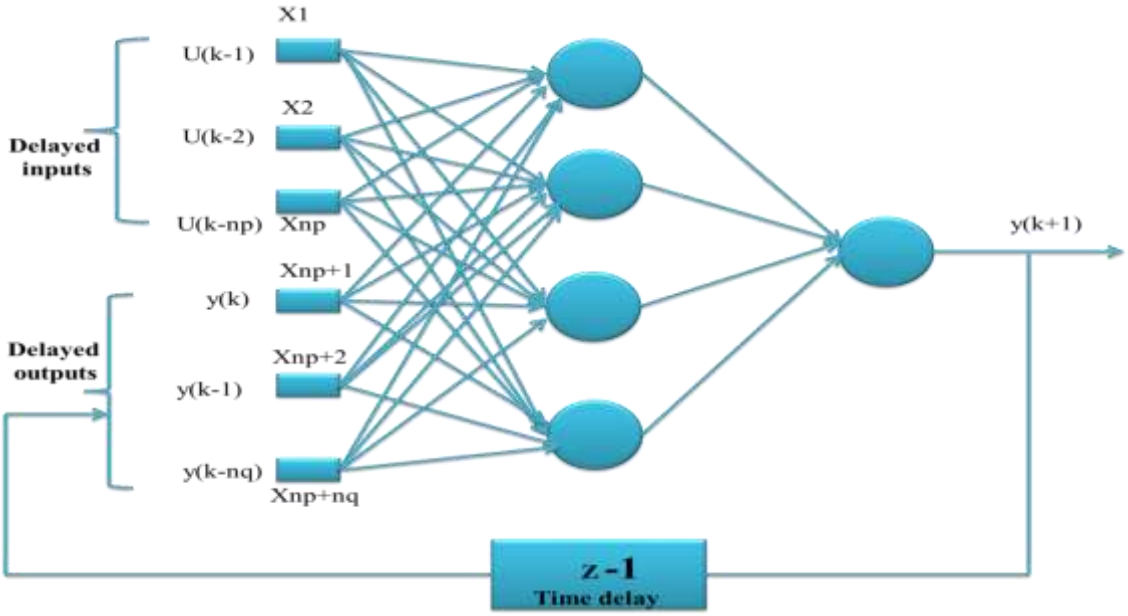

Figure 4. Implantation model diagram for the ANN controller

6. Modes of Operation of Hess

The huge load will be given to the motor in mode one operation, due to which motor demands more power and which will be sent from UC. The controlled signals are formed to switch S_3 and there are no signals produced to switches S_1 and S_2 which starts the operation of BDC (boost). So entire power can flow from UC to the motor. The SOC of battery and output voltage of the PV panel can decide the CS's ON/OFF condition, based on those switches action battery charging and discharging periods are decided. Which is clear from figure 5(a).

In mode-II, the controlled switching signals are produced to both the converters that are BDC and UDC, which means switches S_1, S_3 are in-active state and S_2 in OFF state. The power demanded by the motor can be fulfilled by battery plus UC. During this mode of operation, UC supports the battery by reducing the extra load on the battery.

The electric motor needs the average power in mode three operation which indicates that entire power can be given by the battery itself. The BDC does not operate, whereas UDC can get the pulse signals to connect the battery to the electric motor. Based on the operation BDC and UDC switch S_1 is in ON position and S_2, S_3 are in OFF state.

During mode-IV, EV is operating under no-load or light load, due to which the controlled signals are formed to both UDC and BDC. Here BDC working as a buck to charge the UC whereas UDC working as a boost to supply power to the motor as well UC.

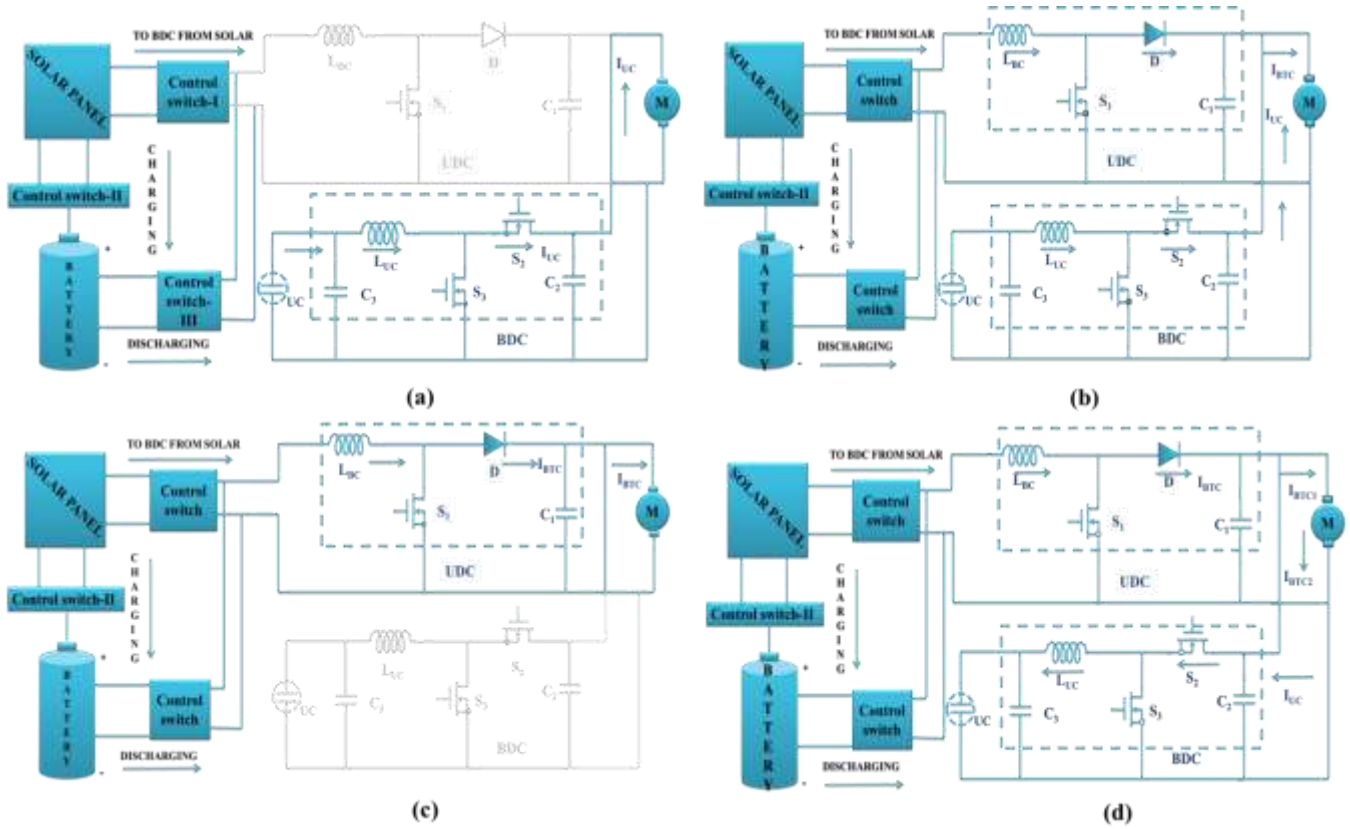

Figure 5. Converter circuit diagram with a solar panel (a) model mode-I (b) model mode-II (c) model mode-III (d) model mode-IV

7. Control Strategy (With MFB and ann ControllersS) Approach

Figure 6 representing the flow chart of the proposed control method. The suggested method organized mainly based on the speed parameter of the motor, which means the speed of the motor playing a vital role during the transition of the energy sources. The transition of energy sources is examined mainly in four load conditions. In the first mode of operation, the controlled switching signals are produced to only S_3. Similarly, in the second mode of operation, the controlled signals are produced to switches S_1 and S_3. In the same way in mode three operation signals are produced to the only S1, and similarly, in the last mode of operation, the controlled switching signals are produced to S1 and S_2. All those controlled signal productions happened because of MFB combined with the ANN controller. From those two controllers, the ANN is used for the production of the switching signals whereas MFB is used for controlling the switching signals. So, the combination of both the controllers makes them smooth and precise switching between energy sources present in HESS.

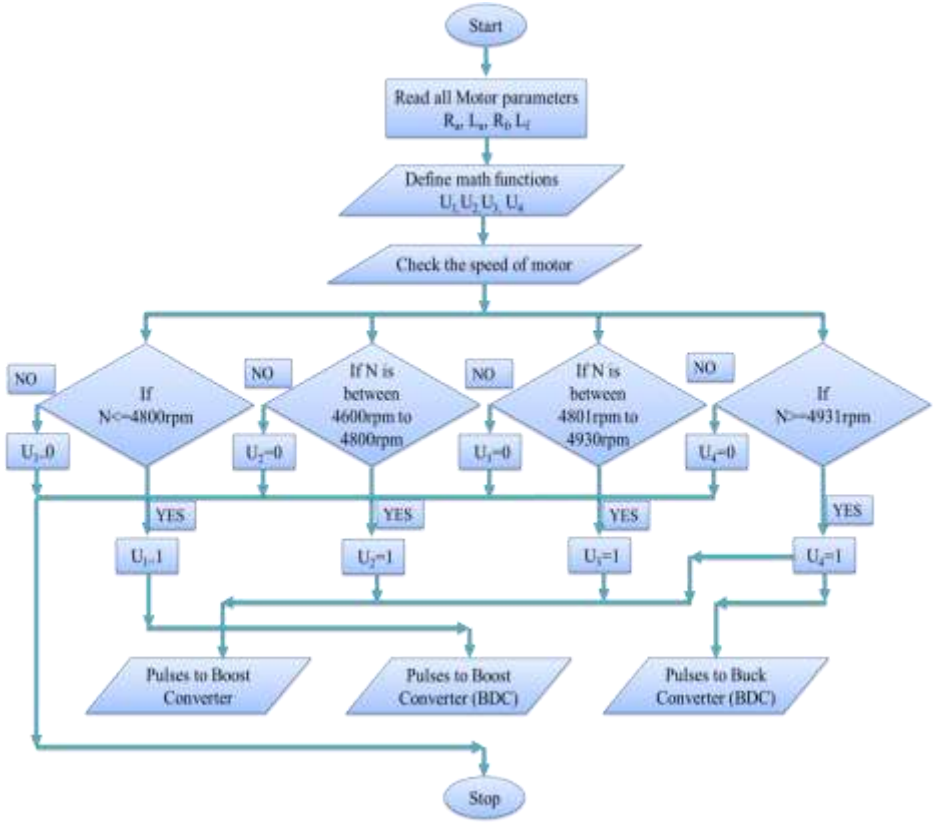

Figure 6. Flowchart representation of the proposed control strategy

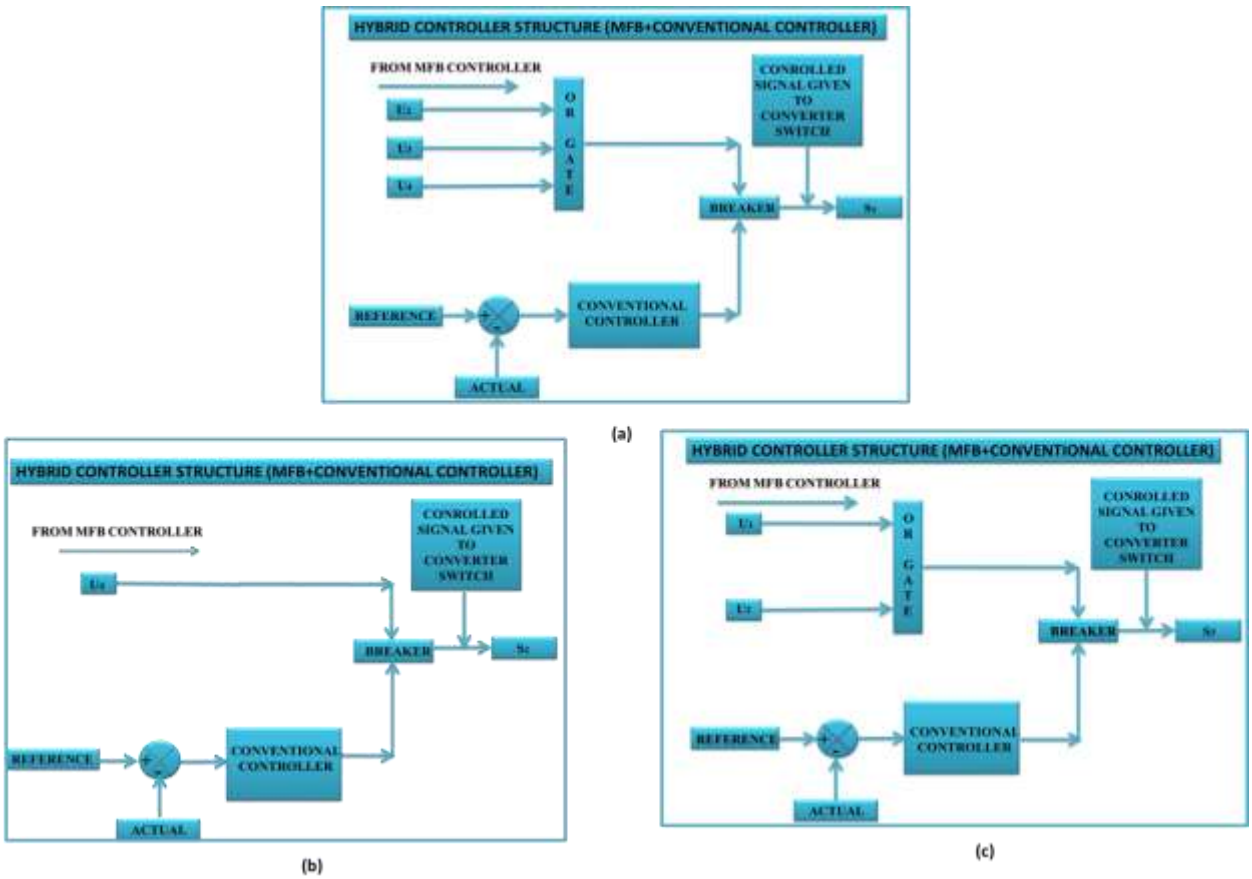

Figure 7. Block diagram representation related to the production of pulse signals to (a) Switch S_1 (b) Switch S_2 (c) Switch S_3 by the designed MFB plus ANN controller

Control strategy scheme can be implemented as follows

x = input of MFB controller which is a variable

y = output variable vector of MFB controller

$$\boldsymbol{y = f(x)\ then}$$
$$\boldsymbol{f(x) = y_0\ when\ x \leq a}$$
$$\boldsymbol{f(x) = y_0, y_1 when\ b \leq x \leq c}$$
$$\boldsymbol{f(x) = y_2\ when\ x \leq d}$$
$$\boldsymbol{f(x) = y_3 when\ x \geq e}$$

Here $\boldsymbol{a, b\ c, d, e}$ are different variable values of "which are given to MFB controller as an input. And $\boldsymbol{y_0 y_1 y_2\ and\ y_3}$ are output vectors of the MFB controller corresponding to input values of "x".

Pulse signal to switch S_1: if $\boldsymbol{y_1 or\ y_2\ or\ y_3}$ of MFB controller present then pulse signals have been given to switch S_1.

Pulse signal to switch S_2: if $\boldsymbol{y_3}$ of MFB controller present case then the pulse signal has been given to the switch S_2.

Pulse signal to switch S_3: if $\boldsymbol{y_0 or\ y_1}$ of MFB controller present then the pulse signal can be generated to the switch S_3.

8. Matlab/Simulink Model Results

8.1 Mode-I operation results

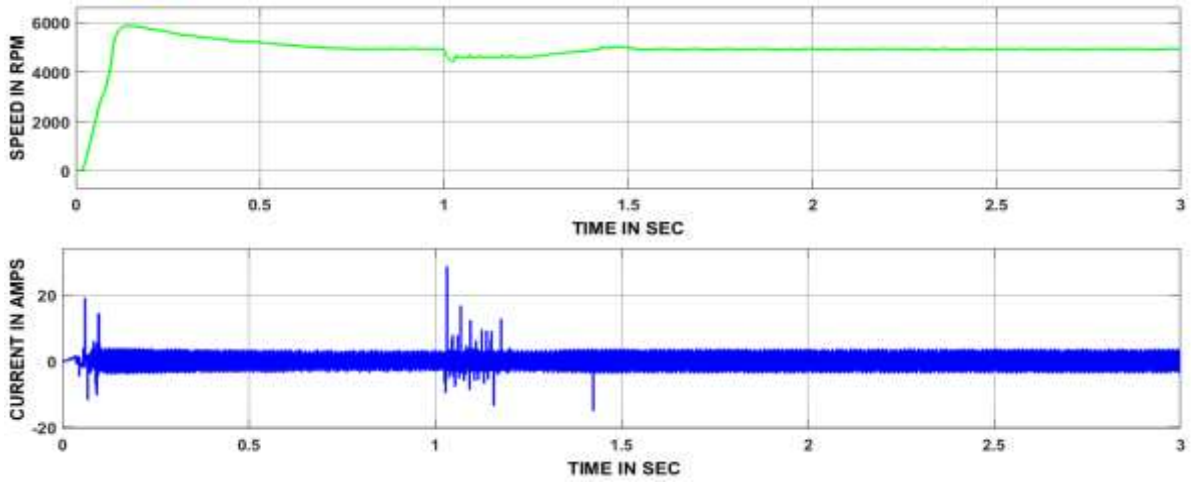

Figure 8. Output responses of the motor corresponding to mode one

Generally, starting time motor demands huge current than its rated value, in the same way, the speed of the motor also reaches more due to peak overshoot. The speed of an electric motor reached a steady-state value before 0.6 sec only. So, during starting the motor can start with the support of UC only because during starting motor requires more power. Thereafter motor draws supply form both the sources, after some time the battery feed both UC and load. At 1sec load applied, due that the speed reduced to $\leq$4600 rpm and correspondingly current value raised drastically. After that, the electric motor attained normal state within 0.4 sec using the considered controller.

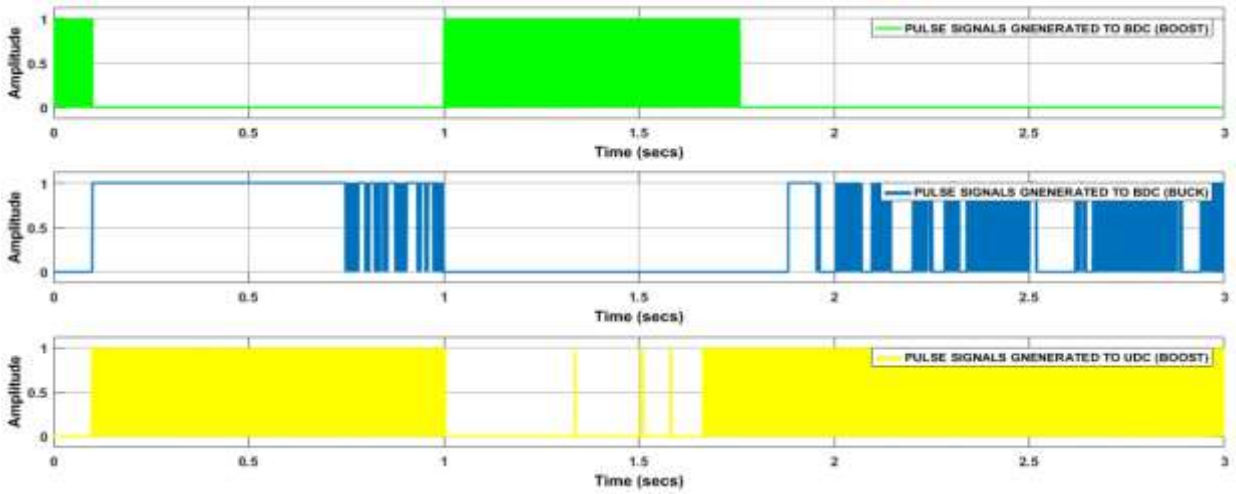

Figure 9. Controlled pulses produced to DC-DC converters

During the start, UC provides energy to the motor, so at this situation controlled pulses are formed to BDC (boost). Thereafter, motor speed reaches between 4600 rpm to 4800 rpm, then the two sources collectively provide power to motor this initiates the operation of BDC (boost) and UDC (boost). After 0.1-sec battery provides the essential power to the motor and UC till load applied, this starts the action of BDC (buck) and UDC (boost). At 1 sec load applied, due that the speed of the motor reduces to $\leq$4600 rpm, this initiates the BDC (boost) and there are no pulse signals produced to UDC, this will continue up to that motor reached a steady-state value. Thereafter again pulse signal generation changed to BDC (buck) and (UDC)boost. All discussed variation in BDC, as well as UDC, clearly observed from figure 9.

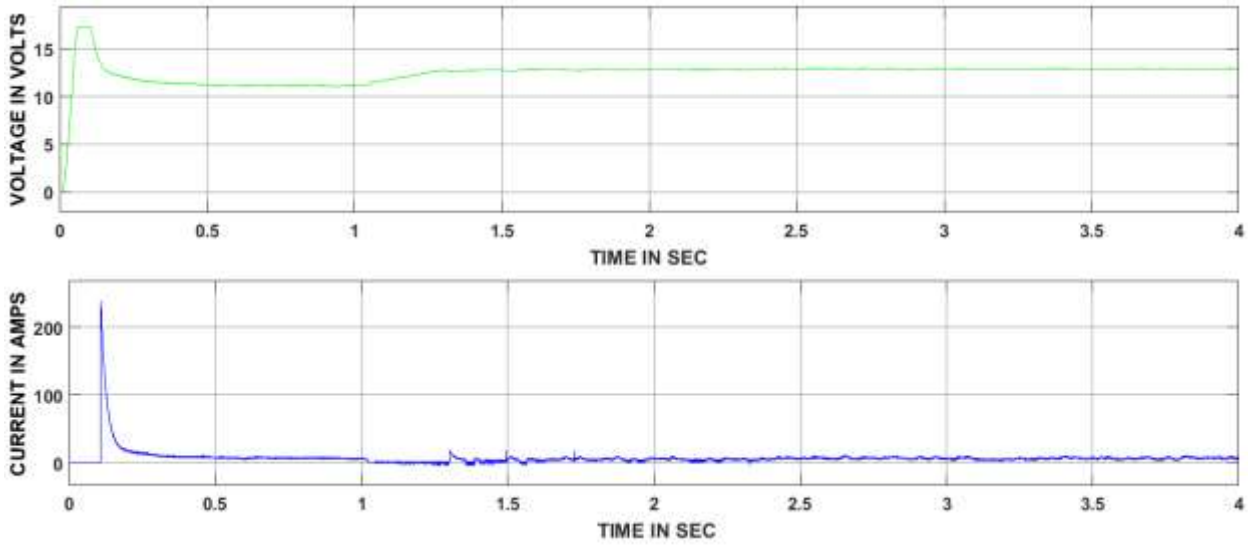

Figure 10. UDC output voltage and current waveforms, mode-I

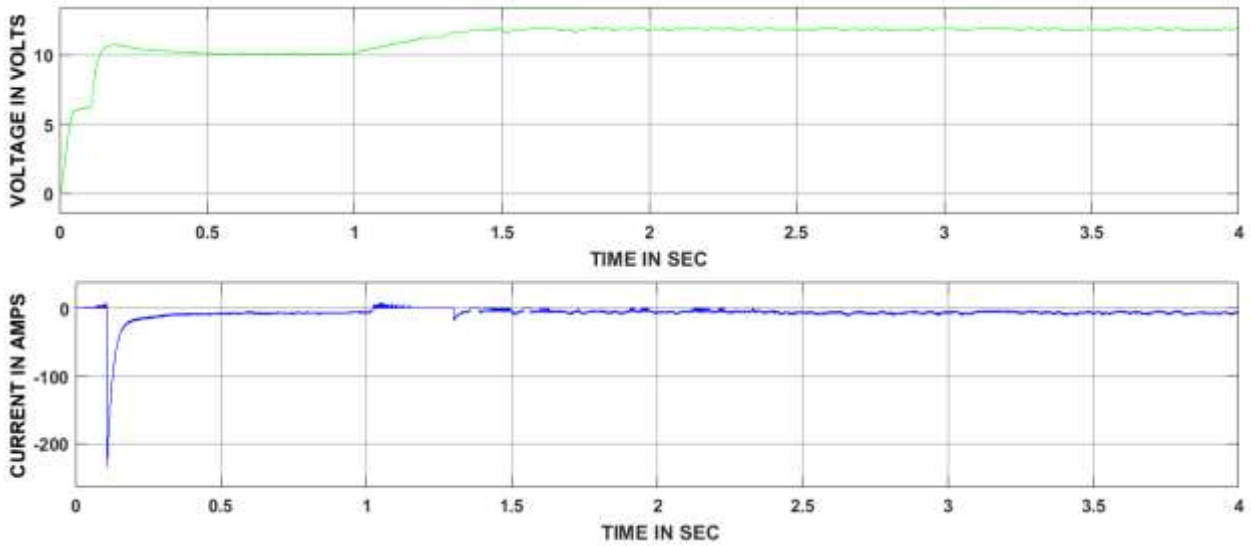

Figure 11. BDC output voltage and current waveforms, mode-I

8.2 Mode-II operation results

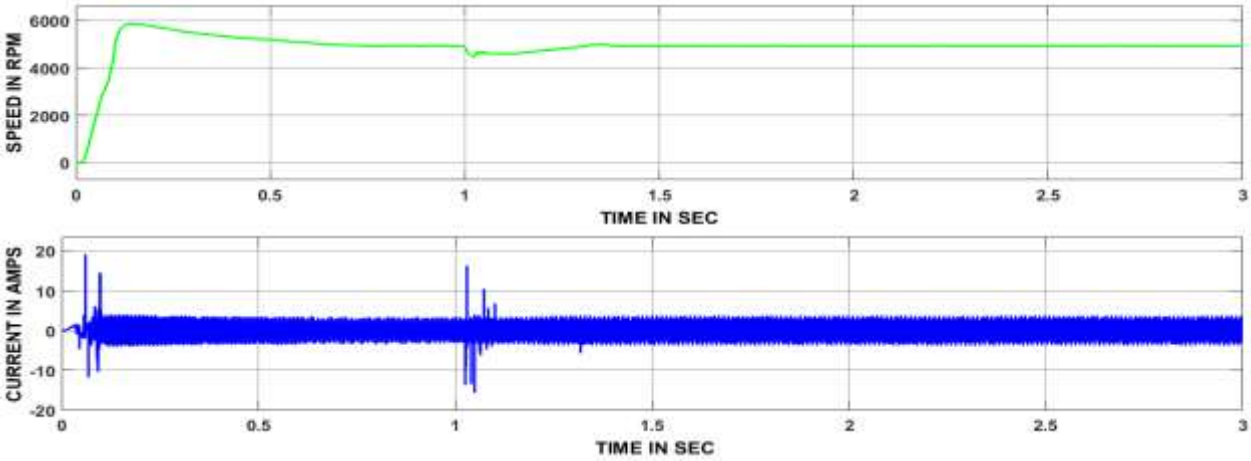

Figure 12. Output responses of the motor corresponding to mode two

At 1sec load applied, due to which the motor speed reduced between 4600 rpm to 4800 rpm and correspondingly current value raised. After that, the electric motor attained normal state within 0.3 sec using the considered controller.

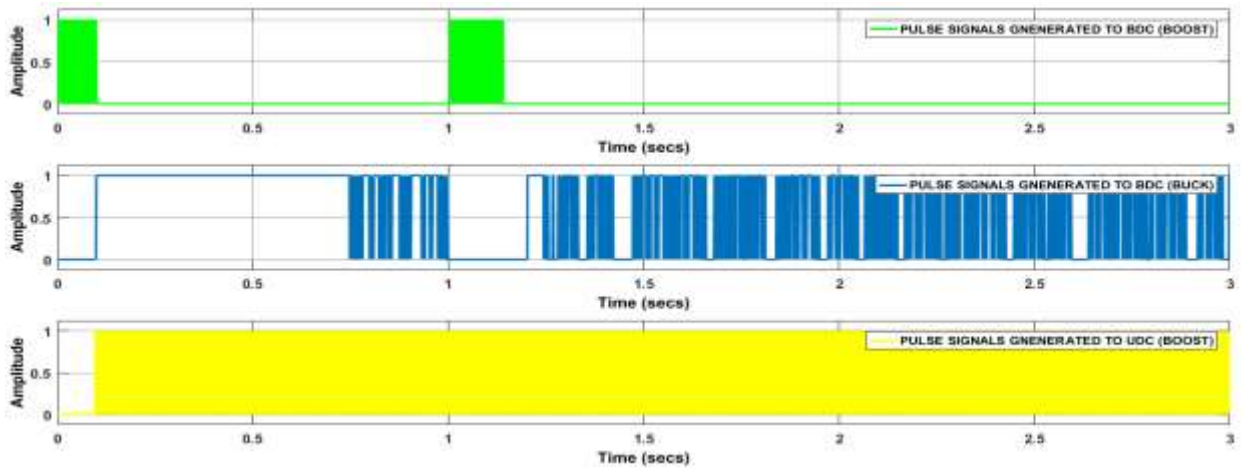

Figure 13. Controlled pulses produced to DC-DC converters

At 1 sec load applied due that the speed of the motor reduces between 4600 rpm to 4800 rpm, this initiates the BDC (boost) and UDC (boost), this will continue up to that motor reached a steady-state value. Thereafter again pulse signal generation changed to BDC (buck) and (UDC)boost.

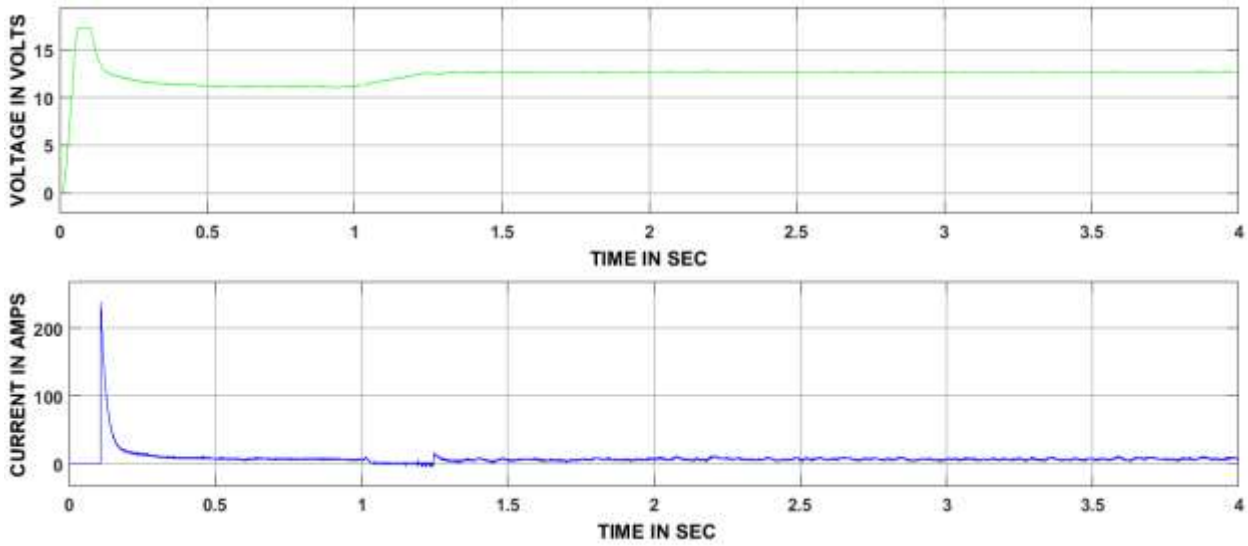

Figure 14. UDC output voltage and current waveforms, mode-II

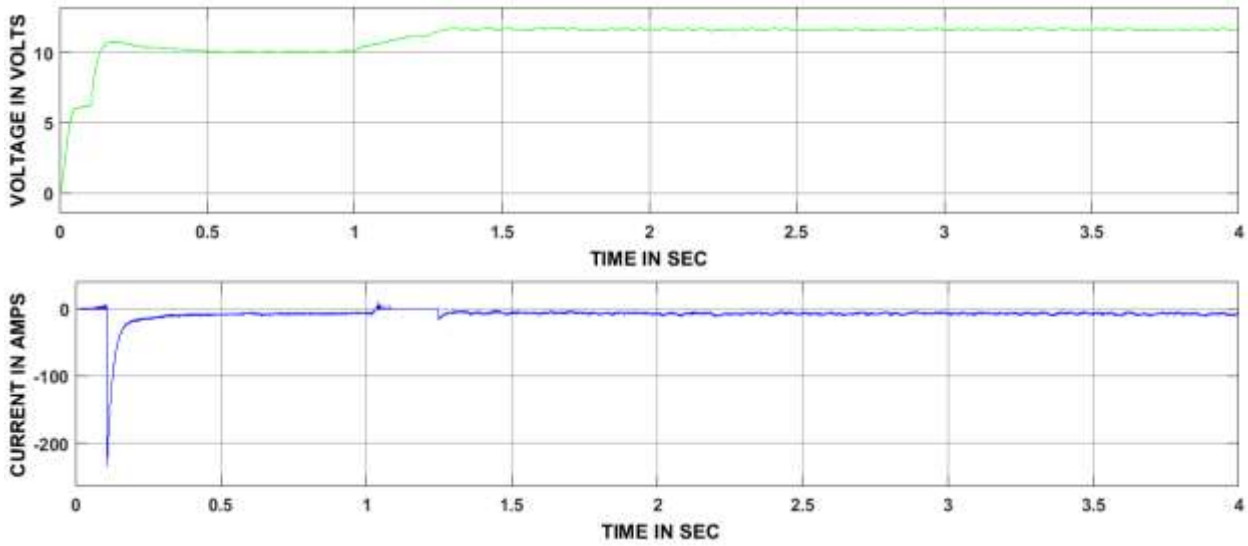

Figure 15. BDC output voltage and current waveforms, mode-II

8.3 Mode-III operation results

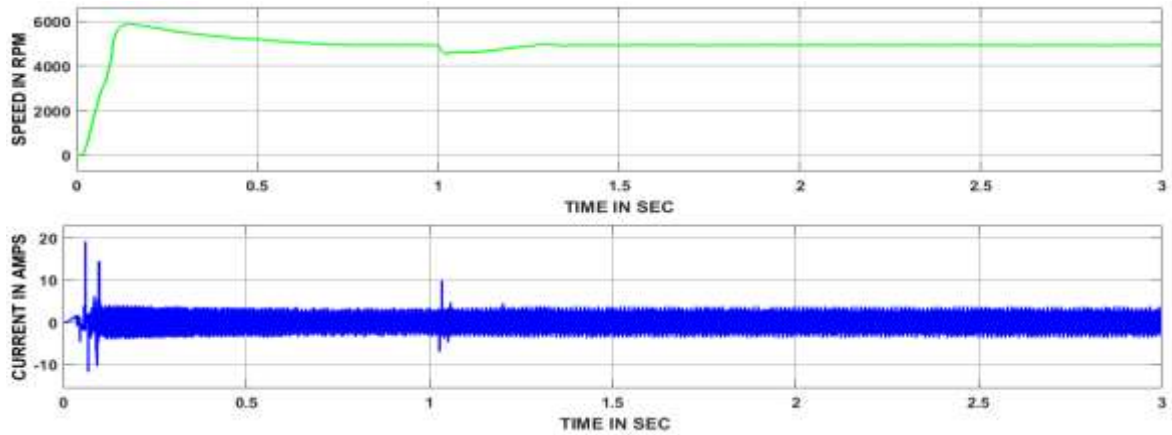

Figure 16. Output responses of the motor corresponding to mode three

At 1sec rated load applied, due that motor speed reduced between 4801 rpm to 4930 rpm and correspondingly current value raised. After that, the electric motor attained the original state within 0.25 sec using the considered controller.

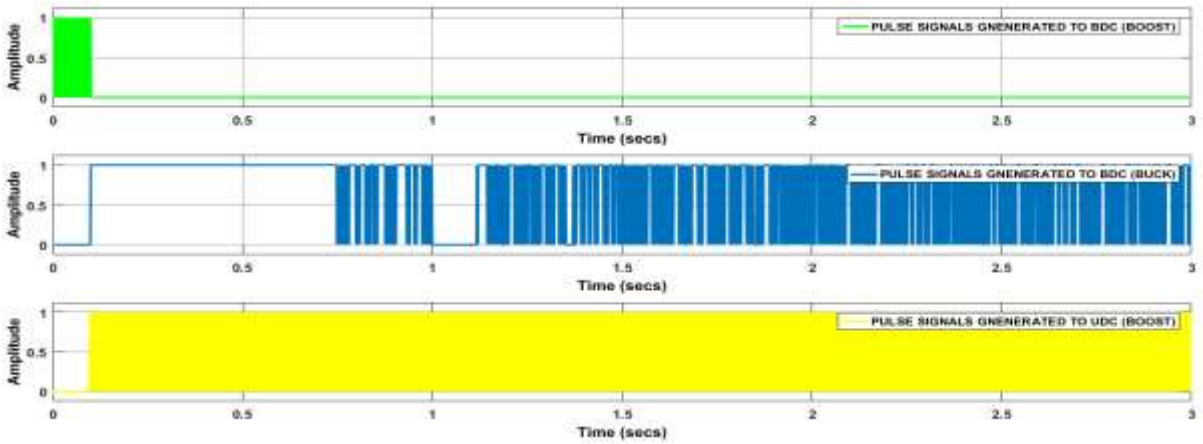

Figure 17. Controlled pulses produced to DC-DC converters

At 1 sec load applied due that the speed of the motor reduces between 4801 rpm to 4930 rpm, this starts the UDC (boost) and there are no pulse signals produced to BDC, this will continue up to that motor reached a steady-state value. Thereafter again pulse signal generation changed to BDC (buck) and UDC (boost).

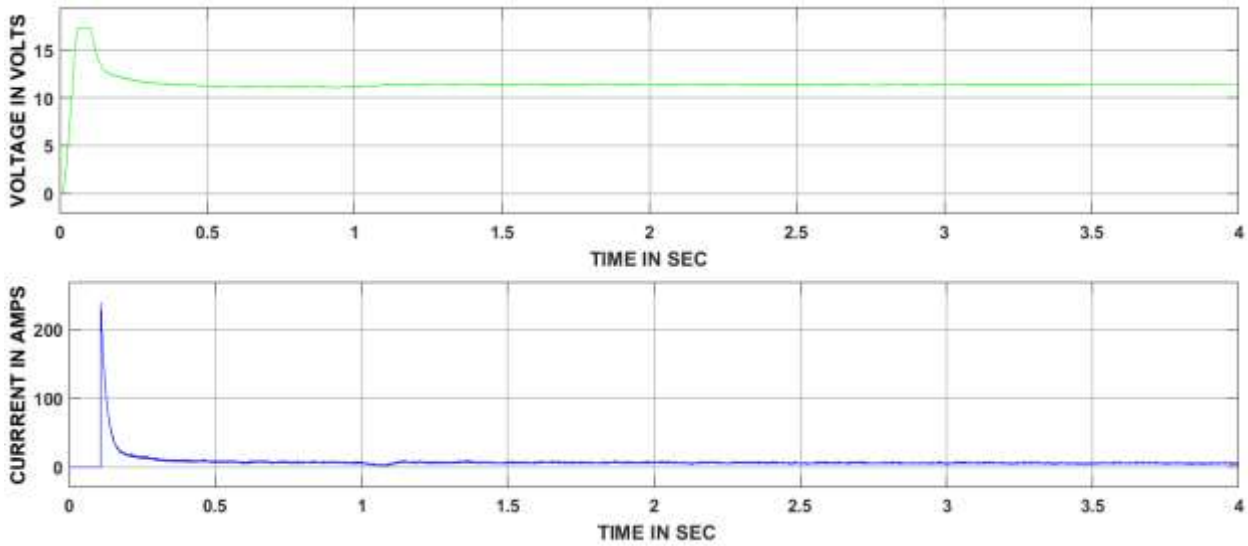

Figure 18. UDC output voltage and current waveforms, mode-III

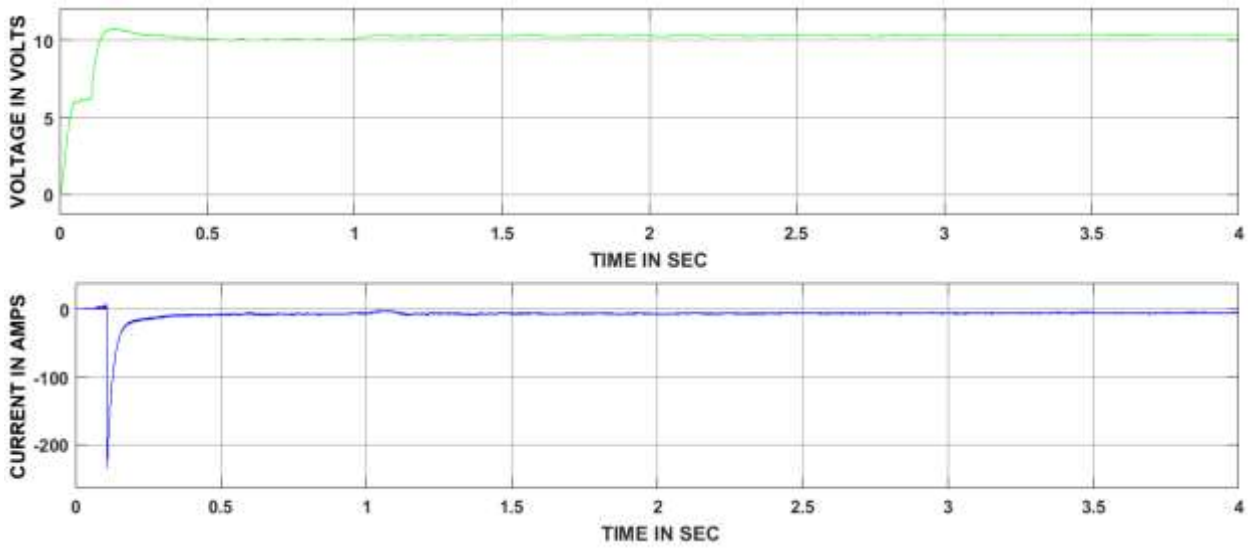

Figure 19. BDC output voltage and current waveforms, mode-III

8.4 Mode-IV operation results

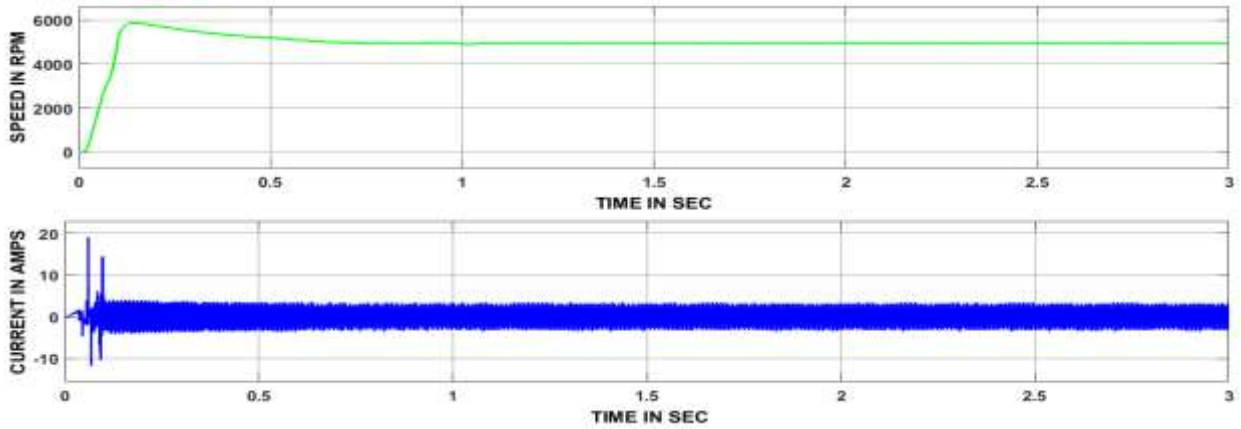

Figure 20. Output responses of the motor corresponding to mode four

No-load has been applied in mode-IV operation. Generally, starting time motor demands huge current than its rated value, in the same way, the speed of the motor also reaches more due to peak overshoot. The speed of an electric motor reached a steady-state value before 0.6 sec only. So, during starting the motor can start with the support of UC only because during starting motor requires more power. Thereafter motor draws supply form both the sources, after some time the battery feed both UC and load. In this mode, no-load is applied, so there are no current and speed response changes are observed after the motor got the normal-state position.

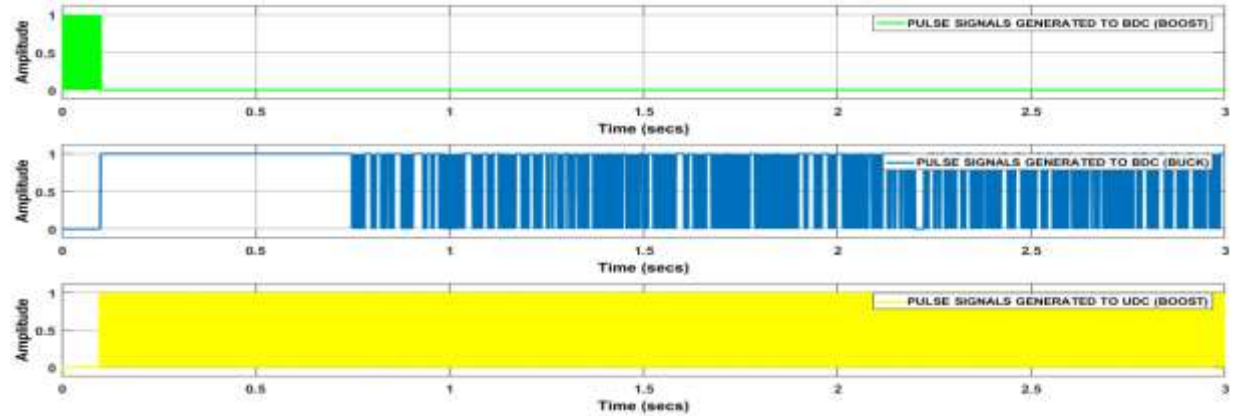

Figure 21. Controlled pulses produced to DC-DC converters

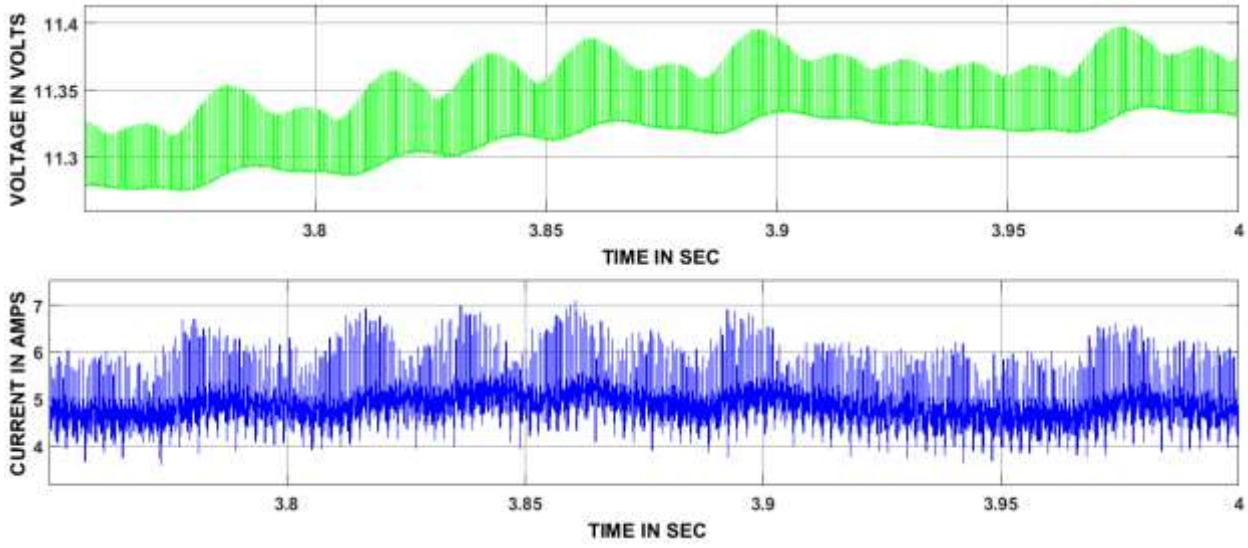

Figure 22. UDC output voltage and current waveforms, mode-IV

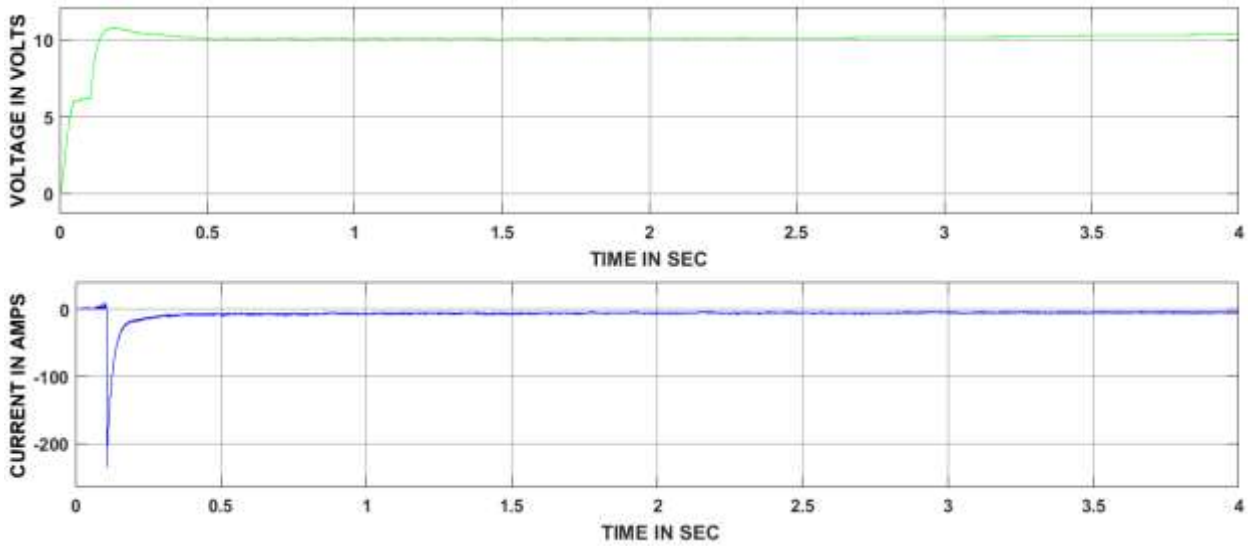

Figure 23. BDC output voltage and current waveforms, mode-IV

Table 2. Performance of the controller based on the load applied

S. No	Mode No.	Time (sec) taken by the controller to attain a normal position after the load	Time (sec) taken by the controller to attain a normal position at starting	Raised current (Amps) value due to the corresponding load	Raised current (Amps) value during starting	Speed (rpm) value corresponding to the applied load
1	Mode-I	0.4	0.6	24	20	4200
2	Mode-II	0.3	0.6	18	20	4650
3	Mode-III	0.25	0.6	10	20	4850
4	Mode-IV	Load free	0.6	2	20	5000

8.5 Battery Parameters

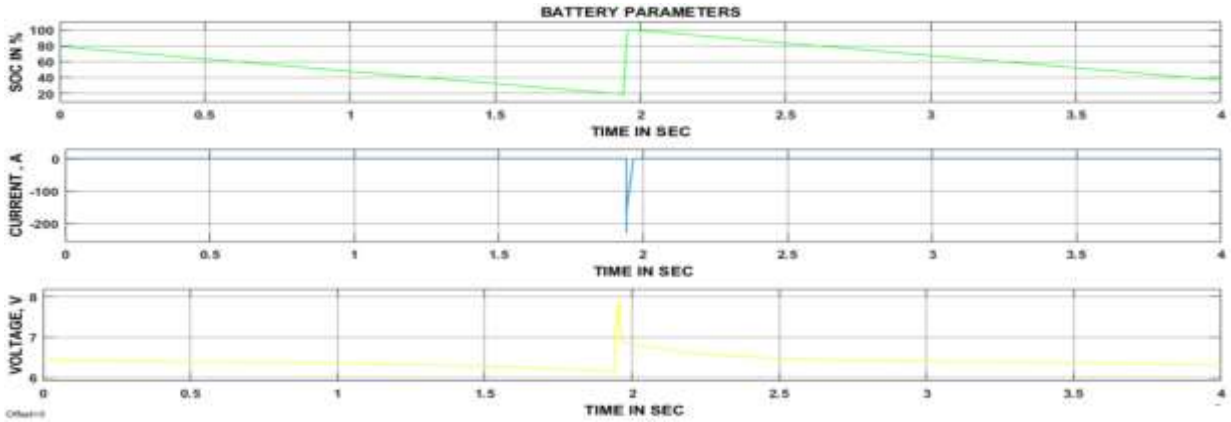

Figure 24. Variations present in different battery parameters

Figure 24 shows, SOC, voltage, and current values of the battery during charge and discharge timings. The negative current of the battery indicates the charge period whereas positive current shows the discharging period. Corresponding to the voltage levels of the battery, SOC value also changes which is clear from figure 24. In this work, the battery gets charged when the SOC is less than 20%.

8.6 Solar Panel Parameters

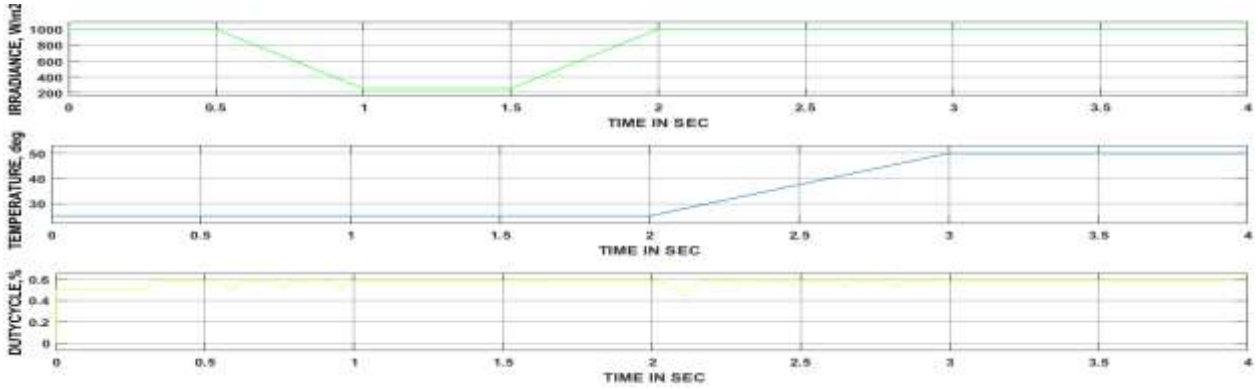

Figure 25. Variations present in different PV cell parameters

Figure 25 representing the irradiance, temperature, and duty cycle curve of the PV panel. The output voltage value changes based on temperature and irradiance availability. Here the duty cycle of the converter changes corresponding to the load requirement. In the power at different voltage levels are obtained using the temperature range from 250c to 500c.

9. Conclusions

Based on the driver requirement a new control technique was designed to switch the energy sources of the EV. The considered MFB controller has regulated the pulses produced by the ANN controller act in accordance with the speed of the motor. From the suggested two controllers MFB played a vibrant role during the transition of sources of HESS by taking the motor speed as the base. The hybrid controller was made by joining the MFB controller with the ANN controller; thereafter this combination was applied to the main circuit in four modes and obtained sensible results. The battery used in the circuit is a rechargeable one and get charged from the PV cell, and also discharged the same amount of power depending upon the control switches action as well as the SOC of the battery. Battery charging and discharging plots are presented in the simulation and results section along with solar panel parameters. The performance analysis is done by taking time specification as a measure and tabulated in the conclusion section.

Table 3. Performance assessment of controllers corresponding to time-domain specifications

Controller	Specifications				
	Delay time (sec)	Rise time (sec)	Peak time (sec)	Settling time (sec)	Maximum peak overshoot (%)
MFB with ANN	0.07	0.9	0.15	0.9	20

References

Chaudhari, K., Ukil, A., Kumar, K. N., Manandhar, U., & Kollimalla, S. K. (2018). Hybrid optimization for economic deployment of ESS in PV-integrated EV charging stations. IEEE Transactions on Industrial Informatics, 14(1), 106-116.

Duan, C., Wang, C., Li, Z., Chen, J., Wang, S., Snyder, A., & Jiang, C. (2018). A solar power-assisted battery balancing system for electric vehicles. IEEE transactions on transportation electrification, 4(2), 432-443.

Ghiassi-Farrokhfal, Y., Kazhamiaka, F., Rosenberg, C., & Keshav, S. (2015). Optimal design of solar PV farms with storage. IEEE Transactions on Sustainable Energy, 6(4), 1586-1593.

Golchoubian, P., & Azad, N. L. (2017). Real-time nonlinear model predictive control of a battery-supercapacitor hybrid energy storage system in electric vehicles. IEEE Transactions on Vehicular Technology, 66(11), 9678-9688.

Hu, S., Liang, Z., & He, X. (2016). Ultracapacitor-battery hybrid energy storage system based on the asymmetric bidirectional Z-source topology for EV. IEEE Transactions on Power Electronics, 31(11), 7489-7498.

Keil, P., Englberger, M., & Jossen, A. (2016). Hybrid energy storage systems for electric vehicles: An experimental analysis of performance improvements at subzero temperatures. IEEE Transactions on Vehicular Technology, 65(3), 998-1006.

Khan, S., Ahmad, A., Ahmad, F., Shafaati Shemami, M., Saad Alam, M., & Khateeb, S. (2018). A comprehensive review on solar powered electric vehicle charging system. Smart Science, 6(1), 54-79.

Li, J., Zhang, M., Yang, Q., Zhang, Z., & Yuan, W. (2016). SMES/battery hybrid energy storage system for electric buses. IEEE Transactions on Applied Superconductivity, 26(4), 1-5.

Liu, N., Chen, Q., Lu, X., Liu, J., & Zhang, J. (2015). A Charging Strategy for PV-Based Battery Switch Stations Considering Service Availability and Self-Consumption of PV Energy. IEEE Trans. Industrial Electronics, 62(8), 4878-4889.

Mesbahi, T., Rizoug, N., Bartholomeüs, P., Sadoun, R., Khenfri, F., & Le Moigne, P. (2017). Optimal Energy Management for a Li-Ion Battery/Supercapacitor Hybrid Energy Storage System Based on a Particle Swarm Optimization Incorporating Nelder–Mead Simplex Approach. IEEE Transactions on Intelligent Vehicles, 2(2), 99-110.

Shen, J., & Khaligh, A. (2015). A supervisory energy management control strategy in a battery/ultracapacitor hybrid energy storage system. IEEE Transactions on Transportation Electrification, 1(3), 223-231.

Shen, J., & Khaligh, A. (2016). Design and real-time controller implementation for a battery-ultracapacitor hybrid energy storage system. IEEE Transactions on Industrial Informatics, 12(5), 1910-1918.

Trovao, J. P., Roux, M. A., Ménard, É., & Dubois, M. R. (2017). Energy-and power-split management of dual energy storage system for a three-wheel electric vehicle. IEEE Trans. Veh. Technol, 66.